

## Memristor Hybrid Model for Nonlinear Analog Circuit Design

G.M. Tornez-Xavier<sup>1</sup>, M.A. Gutiérrez-Mondragón<sup>1</sup>, L.M. Flores-Nava<sup>1</sup>,  
 F. Gómez-Castañeda<sup>1</sup>, J.A. Moreno-Cadenas<sup>1</sup>

<sup>1</sup>Department of Electrical Engineering, CINVESTAV-IPN, Mexico City, Mexico

Phone (52) 55 5747 3800 Ext. 6261

E-mail: {gtornez, mario.gutierrez, lmflores, fgomez, jmoreno} @cinvestav.mx

**Abstract** — In this work we present the realization of a hybrid model (hardware-software) for memristors based on the nonlinear dopant model for three window functions: Strukov, Joglekar and Prodromakis. Proposing a methodology that allows us to design nonlinear analog circuits with memristors in an easier and faster way using the tools of Simulink, Simscape and System Generator. In addition, we tested the functionality of our hybrid model through the design of an oscillator without reactance, also verifying the effectiveness and scope of our proposed methodology.

**Keywords** — memristor, nonlinear ion drift model, windows functions, oscillators, FPGA.

### I. INTRODUCTION

In 1971, Leon O. Chua [1] considered the existence of a new passive element of circuits of two terminals called memristor (memory and resistor). He observed that by combining in pairs the four fundamental circuit variables: voltage ( $v$ ), current ( $i$ ), magnetic flux ( $\phi$ ), and charge ( $q$ ) six mathematical relationships were obtained, where the relationship between flux and charge was still unknown Fig. 1.

In 2008, Stanley Williams and his team of HP (Hewlett-Packard Laboratories) fabricated the memristor for the first time with the aim of creating nano switches whose resistance ranged from a minimum value  $R_{ON}$  to a maximum value  $R_{OFF}$  [2]. Since then the interest of the memristor in the field of non-volatile memories [3], programmable analog electronics [4] and neural networks [5] has drawn attention. For this reason there is a need to create models that reproduce their physical behavior for use in the creation of circuits and systems. There are also works in which the main interest is the creation of a memristor emulator in FPGA (Field Programmable Gate Array) [6].

This article focuses on the creation of a hybrid model of the HP model for three window functions: Strukov, Joglekar and Prodromakis implemented in a FPGA or programmable logic device using: Simulink, Simscape and System Generator working environment. Finally, the design of an analog oscillator without reactance is presented to demonstrate the effectiveness of our hybrid model.

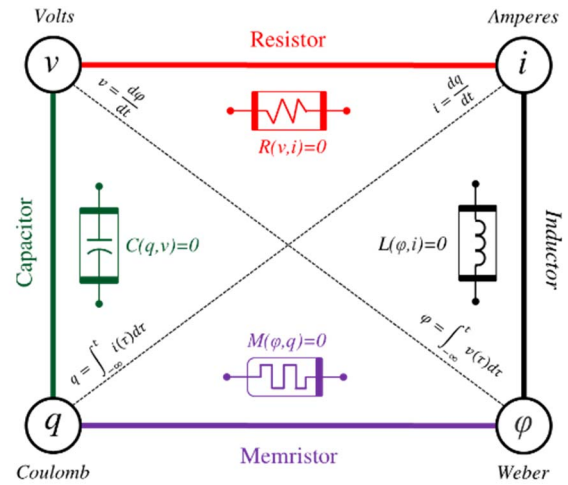


Fig. 1 Model of the relationship between the four fundamental variables in circuit theory.

#### A) Linear ion drift model

Fig. 2 shows the structure of the physical model of the memristor device consisting of two regions: a region doped with oxygen vacancies ( $TiO_{2-x}$ ), which acts as a conductor and another region without doping ( $TiO_2$ ) that acts as a dielectric. These regions are between two platinum contacts: the doped region and the non-doped region that can be seen as two variable resistors connected in series.

When a positive voltage is applied the oxygen vacancies of the  $TiO_{2-x}$  layer are repelled, moving towards the non-doped  $TiO_2$  layer causing an increase in the conductivity throughout the device until reaching the  $R_{ON}$  state when  $w = D$ . When a negative voltage is applied the oxygen vacancies are attracted and pushed out of the  $TiO_{2-x}$  layer increasing the resistance of the whole device until it reaches the  $R_{OFF}$  state when  $w = 0$ . If the voltage of the device is suppressed the oxygen vacancies do not move causing the resistive value to remain intact and unalterable, so that the memristor is able to remember its last value of voltage or current applied. The thickness of the device is represented by  $D$  and  $w$  is the width of the doped region which is modulated by the amount of charge passing through the device.

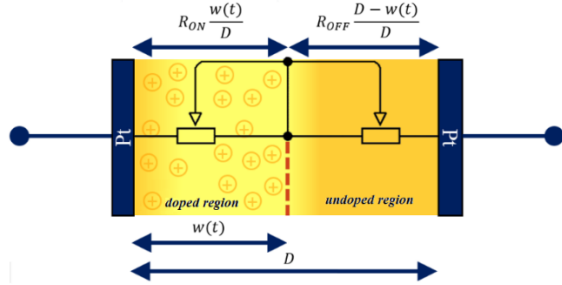


Fig. 2 Pt/TiO<sub>2</sub>/Pt structure of HP® Memristor.

The total resistance of the memristor  $R_{MEM}$  is represented by (1) where  $x$  is the normalized width of the doped region.

$$R_{MEM}(x) = R_{ON} \frac{w(t)}{D} + R_{OFF} \left(1 - \frac{w(t)}{D}\right) \quad (1)$$

$$x = \frac{w}{D} \in [0,1] \quad (2)$$

The speed of the boundary between the doped and the non-doped region is represented by  $dx/dt$  where  $\mu_v$  is the average ion mobility in m<sup>2</sup>V<sup>-1</sup> s<sup>-1</sup>.

$$\frac{dx(t)}{dt} = \mu_v \frac{R_{ON}}{D^2} i(t) \quad (3)$$

And the current-voltage relationship of the memristor is established by Ohm's law.

$$v(t) = (R_{ON}x + R_{OFF}(1 - x))i(t) \quad (4)$$

### B) Nonlinear ion drift model

In this model,  $dx/dt$  varies in a non-linear way, because when a small voltage is applied to the memristor it produces a large electric field causing a non-linear ion drift. In addition, Strukov found that when the boundary between the doped and the non-doped region reaches either end of the device  $w = 0$  or  $w = D$  the boundary velocity is zero, producing non-linearities in the ionic transport [2]. To solve this problem, a window function  $f(x)$  is added to the linear model.

$$\frac{dx}{dt} = ki(t)f(x) \quad (5)$$

$$k = \frac{\mu_v R_{ON}}{D^2} \quad (6)$$

### C) Window Function

The window function adds a non-linear behavior at the ends of the device. There are several window functions that have been proposed. Strukov [2] proposed the first window function with the linear model.

$$f(x) = x - x^2 \quad (7)$$

Joglekar and Wolf [7] presented the following function where we have a positive control parameter  $p$  that controls the linearity of the model.

$$f(x) = 1 - (2x - 1)^{2p} \quad (8)$$

Prodromakis [8] has the following window function which has a scalability factor  $j$  that allows  $f(x)$  to be less than or greater than 1 and  $p$  can be any positive real number.

$$f(x) = j(1 - [(x - 0.5)^2 + 0.75]^p) \quad (9)$$

## II. METHODOLOGY

When it comes to the modeling of the memristor in the environment of Simulink, this cannot be treated as a physical element of two terminals since Simulink handles it as a black box with an input for the voltage and an output for the current so it cannot be used in the simulation of electrical systems. To solve this problem Simulink has a tool called Simscape that allows the simulation and modeling of physical systems in different engineering areas: electrical, hydraulic, mechanical etc.

Figure 3 shows the methodology addressed in [9] for the implementation of the nonlinear dopant drift model (5) using Simulink blocks and a potentiometer from the Simscape electrical element library, that physically represents the memristor. In this paper, we present a hybrid option where we work part of the design at hardware level and another at software level.

One way to address this problem is to use the System Generator development tool, which offers a function blocks library that can be implemented in an FPGA device. Because some memristor parameters are too large and others small is necessary to use floating point arithmetic (IEEE 754-2008 standard). Fig. 4 shows the complete diagram with all the blocks used for the realization of the nonlinear ion drift model with the described window functions.

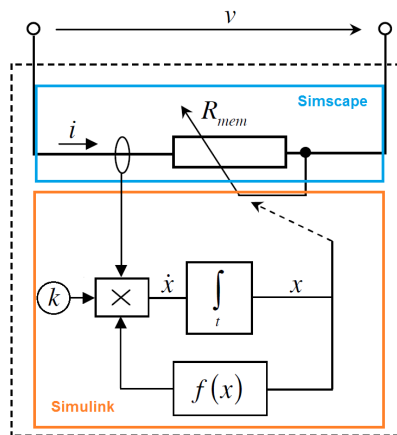


Fig. 3 Scheme of the memristor.

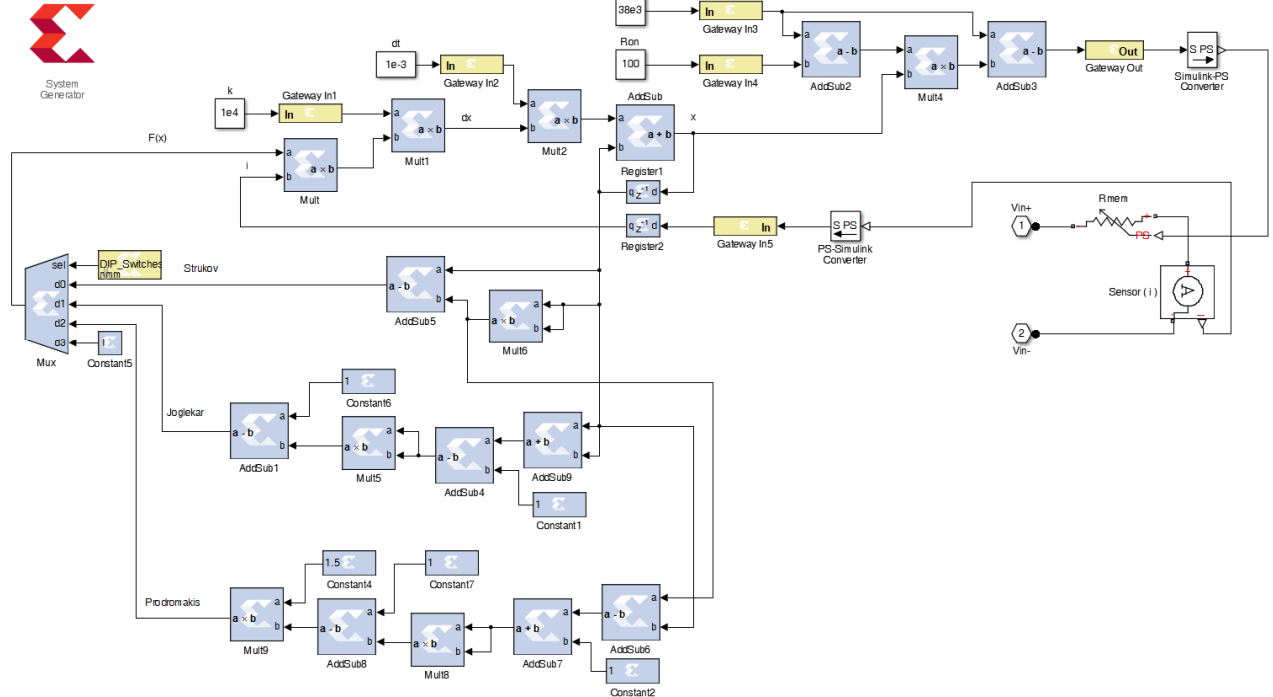


Fig. 4 Complete diagram of the nonlinear dopant model.

The method that allows us to implement the model built in Simulink at Hardware level is using a block called Hardware / Software Co-simulation (JTAG Co-sim). Fig. 5 shows the JTAG Co-sim block where the calculation of the window functions, the  $x$  state variable and the  $R_{MEM}$  memristance value is performed at hardware level, which is transferred to the two-terminal potentiometer of Simscape for having the voltage-current memristor ratio. A Spartan-6E FPGA was used and the logical resources used were: 4308 LUTS, 637 Registers, 40 DSPs and 2 RAMB16B.

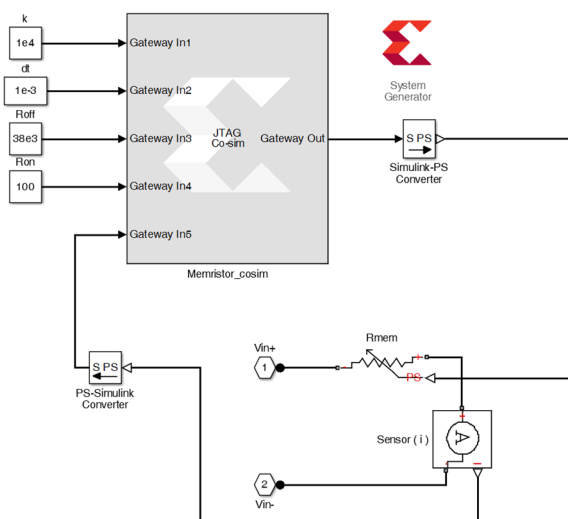


Fig. 5 Diagram of the hybrid model.

### III. HYBRID MODEL TEST

To evaluate the functionality of our hybrid model of the memristor, the Fig. 6 shows the circuit assembled with a sinusoidal signal of 1.0V of peak and frequency of 0.3mHz.

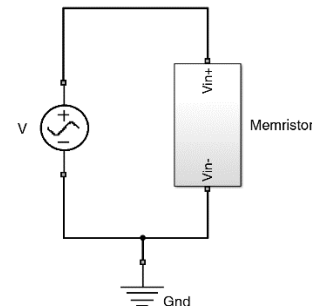


Fig. 6 Measuring circuit with the following parameters:  
 $R_{ON} = 100\Omega$ ,  $R_{OFF} = 38K\Omega$ ,  $k = 1.0 \times 10^4$ ,  $x_{init} = 0.3145$

In Fig. 7 the results of the simulation of the memristor are shown, where for the Strukov function we have a current  $I_{mem} = 41\mu A$  and a variation from  $22K\Omega$  to  $26K\Omega$  for  $R_{mem}$ . In Joglekar there is a control parameter  $p = 1$  where  $I_{mem} = 116\mu A$  and the value of  $R_{mem}$  varies from  $1.8K\Omega$  to  $26K\Omega$ . In Prodromakis we have the control parameters  $p = 2$  and  $j = 1.5$  where  $I_{mem} = 67\mu A$  and  $R_{mem}$  varies from  $6K\Omega$  to  $26K\Omega$  observing that with Joglekar and Prodromakis a greater variation in the resistive value of the memristor can be obtained.

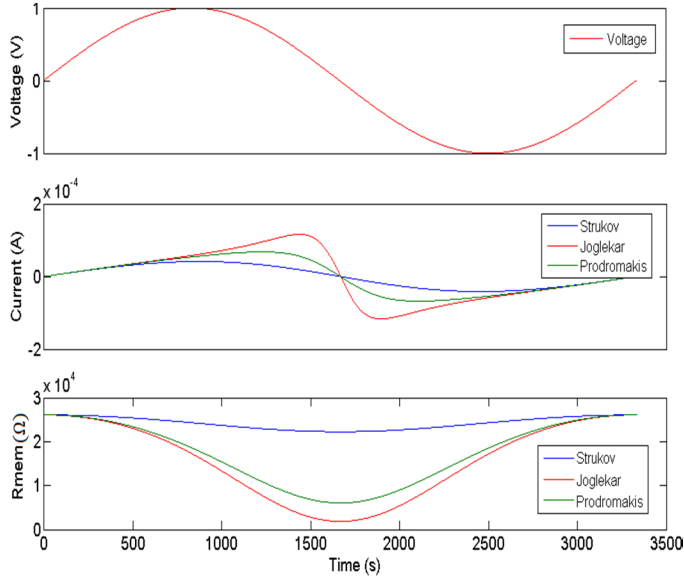


Fig. 7 Transient analysis.

Fig. 8, reproduces the voltage-current relationship of the memristor, the hysteresis function can be compared for all proposed window functions, observing that the waveforms are symmetrical with respect to the origin.

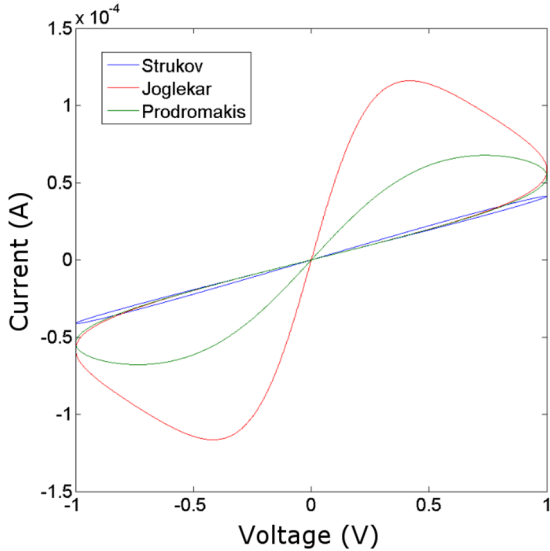


Fig. 8 Voltage-Current relationship of the memristor.

#### IV. MEMRISTOR-BASED APPLICATION

In this article we will perform the analysis of an oscillator without a reactance based on a memristor [10]. According to Fig. 9, the circuit simulates the loading and unloading response of an RC circuit through a voltage divider formed from a resistor and a serial memristor. The control module can be developed with two comparators in parallel, where the output of each serves as input of an AND gate responsible for generating the oscillation.

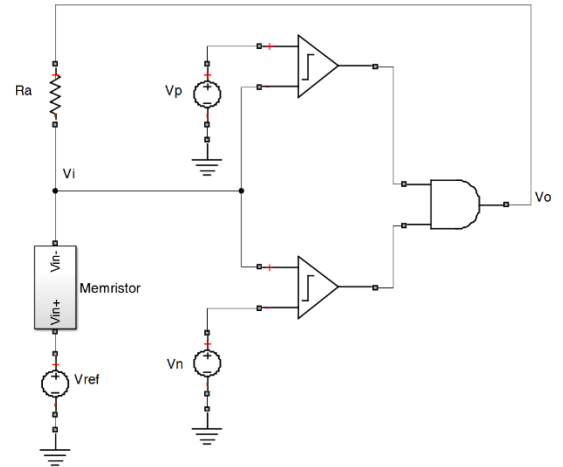


Fig. 9 Oscillator circuit without reactance.

The oscillation function is performed based on the voltage at the  $V_i$  node, however, to facilitate the analysis the voltage in the memristor is considered, which can be described as:

$$V_M(t) = (V_o(t) - V_{ref}) \frac{R_m}{R_m + R_a} \quad (10)$$

The variation of the memristance  $R_M$  is defined based on the polarization voltages of the comparators:  $V_p$  and  $V_n$ , presenting a maximum resistance value in  $R_{Mp}$  and minimum in  $R_{Mn}$ . These values can be determined from (10) as:

$$R_{Mp} = R_a \frac{V_p - V_{ref}}{V_{oh} - V_p}; R_{Mn} = R_a \frac{V_n - V_{ref}}{V_{ol} - V_n} \quad (11)$$

The polarization voltages in the comparators  $V_p$  and  $V_n$  prevent  $R_M$  from acquiring a constant value, due to the border of the regions of the memristor reached some of the ends. In this way,  $R_{Mp}$  and  $R_{Mn}$  should be defined such that the border does not reach the saturation.

$$R_{on} < R_{Mn} < R_{Mp} < R_{off} \quad (12)$$

According to the value of  $R_a$ , the necessary condition for correct circuit oscillation can be obtained by substituting (11) into (12)

$$R_{on} \left( \frac{V_{ol} - V_n}{V_n - V_{ref}} \right) < R_a < R_{off} \left( \frac{V_{oh} - V_p}{V_p - V_{ref}} \right) \quad (13)$$

Regarding the resistance variation in the memristor, the HP model is considered, where the movement of the boundary between the doped and the non-doped region is described, using the state equation.

$$\frac{dx(t)}{dt} = k i(t) f(x) \rightarrow k = \frac{\mu_v R_{on}}{D^2} \quad (14)$$

For the analysis of the oscillator the function of window of Joglekar was used with  $p = 1$ , since, to a greater value in  $p$ , the function becomes linear, presenting an undesired effect in

the analysis of the circuit. To facilitate the development of expressions, the window function can be described as:

$$f(x) = 4x(1-x) \quad (15)$$

The resistance of the memristor is defined according to the sum of the resistances in series with respect to the doped and non-doped region  $R_{MEM}(x) = R_{ON}x + R_{OFF}(1-x)$  which can be defined as:

$$R_{MEM}(x) = R_{OFF} - x(R_{OFF} - R_{ON}) \quad (16)$$

The current flowing through the memristor can be determined analytically from the diagram of Fig. 9.

$$i_m(t) = \frac{V_o(t) - V_{ref}}{R_a + R_{MEM}} \quad (17)$$

Using (17) and the window function of Joglekar, it is possible to obtain a version of the equation of state (18) which will allow to obtain an expression for the calculation of the frequency.

$$\frac{dx}{dt} = \frac{k(V_o(t) - V_{ref})(4x(1-x))}{R_a + R_{OFF} - x(R_{OFF} - R_{ON})} \quad (18)$$

With (18), it is possible to obtain the time the output lasts in high state  $T_H$  and in low state  $T_L$  of the oscillator. Thus, integrating from  $x_{Mp}$  to  $x_{Mn}$  and as a function of time  $T_H$ , considering  $V_o(t) = V_{OH}$  we have:

$$\frac{1}{4k(V_{OH} - V_{ref})} \int_{x_{Mn}}^{x_{Mp}} \left( \frac{R_{OFF} + R_a}{x} + \frac{R_{on} + R_a}{1-x} \right) dx = \int_0^{T_H} dt \quad (19)$$

From this expression,  $x_{Mp}$  and  $x_{Mn}$  correspond to the value of the boundary when the resistance value is  $R_{Mp}$  and  $R_{Mn}$ , respectively. These variables are determined through the equation of the resistance of the memristor (16), clearing the state variable, resulting in:

$$x_{Mp} = \frac{R_{Mp} - R_{off}}{R_{off} - R_{on}} \quad x_{Mn} = \frac{R_{Mn} - R_{off}}{R_{off} - R_{on}} \quad (20)$$

By solving the integral (19) and making the corresponding substitutions, it is possible to obtain an equation of the positive half-cycle of the signal  $T_H$ .

$$T_H = \frac{(R_a + R_{off}) \ln \left( \frac{R_{Mn} - R_{off}}{R_{Mp} - R_{off}} \right) + (R_{on} + R_a) \ln \left( \frac{R_{on} - R_{Mp}}{R_{on} - R_{Mn}} \right)}{4k(V_{OH} - V_{ref})} \quad (21)$$

For the negative half-cycle of the signal, the state equation (18) is integrated from  $x_{Mn}$  to  $x_{Mp}$  as a function of  $T_L$  and with  $V_o(t) = V_{OL}$ .

$$T_L = \frac{(R_a + R_{off}) \ln \left( \frac{R_{Mp} - R_{off}}{R_{Mn} - R_{off}} \right) + (R_{on} + R_a) \ln \left( \frac{R_{on} - R_{Mn}}{R_{on} - R_{Mp}} \right)}{4k(V_{OL} - V_{ref})} \quad (22)$$

Taking into account the ratio of the time in which the signal is active  $T_H$  and its period  $T$ , the expression for the oscillator duty cycle can be obtained as:

$$D = \frac{T_H}{T} \quad (23)$$

From (23) the period  $T$  is determined from the sum of the time in high and low of the signal ( $T = T_H + T_L$ ). And with the reciprocal of the period, the working frequency of the oscillator can be determined as:

$$f = \frac{1}{T_H + T_L} \quad (24)$$

Based on the above expression, it can be noted that the oscillation frequency of the circuit can be controlled by different parameters. For example, by means of the reference voltage, the polarization values in the comparators, etc. But the easiest way to control the oscillation frequency is by means of the resistance  $R_a$ , placed in series with the memristor, since it is an easy and accessible parameter to adjust.

## V. OSCILLATOR RESULTS

Using the developed memristor model, the following data were used:  $R_{ON} = 100\Omega$ ,  $R_{OFF} = 38K\Omega$ ,  $k = 1.0 \times 10^4$ . And the circuit parameters  $V_{OL} = 0V$ ,  $V_{OH} = 2V$ ,  $V_n = 0.5V$ ,  $V_p = 1.75V$  and  $V_{ref} = 1.0V$ . Fig. 10 shows the co-simulation results considering  $R_a = 3k\Omega$  and substituting in (11), the resistance variation expected in the memristor is  $R_{Mn} = 3k\Omega$  and  $R_{Mp} = 9K\Omega$ .

In addition, the oscillation interval for the memristance and the voltage variation in the memristor can be noted, with the switching condition being fulfilled when the input voltage  $V_i$  is equal to  $V_p$  or  $V_n$ . Finally, the output signal with a 50% circuit duty cycle is also shown.

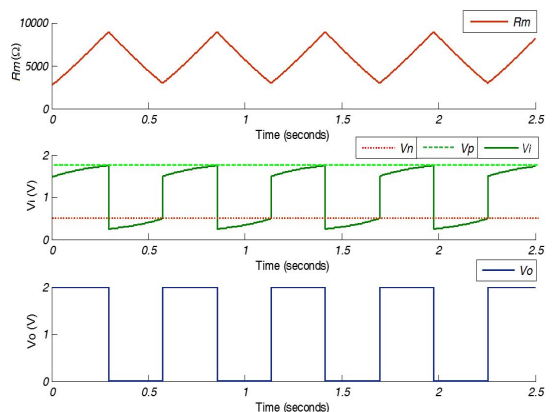


Fig. 10 Results of co-simulation with  $R_a=3k\Omega$

As mentioned, the frequency of the circuit can be controlled through the resistor  $R_a$ , therefore, a sweep from  $1\text{k}\Omega$  to  $12\text{k}\Omega$  was performed to verify the presented analysis. In Fig. 11, a graph of the behavior of the frequency as a function of the variation of the resistance  $R_a$  is shown.

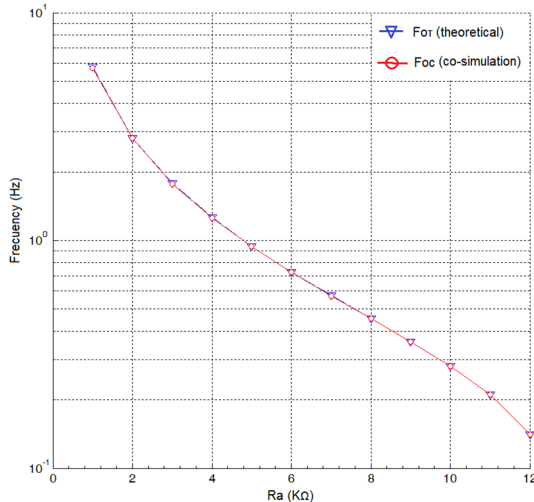


Fig. 11 Graph of the behavior of the frequency

Table 1 shows a comparison of the data obtained from the co-simulation and those obtained theoretically. In addition, the error rate calculated as  $(\text{abs}(F_{0\text{f}} - F_{0\text{c}}) / F_{0\text{f}}) * 100$  is shown, showing a value below 1%. So, it can be mentioned that the deviation of the data obtained in the co-simulation with the expected ones through the mathematical expressions are acceptable.

Table 1. Comparison of theoretical frequency versus co-simulation.

$R_a$ ( $\text{k}\Omega$ )	$F_{0\text{f}}(\text{Hz})$ (theoretical)	$F_{0\text{f}}(\text{Hz})$ (co-simulation)	Error (%)
1	5.7899	5.7471	0.7392
2	2.8205	2.8089	0.4112
3	1.7879	1.7793	0.4810
4	1.2626	1.2594	0.2534
5	0.9436	0.9416	0.2119
6	0.7286	0.7278	0.1097
7	0.5730	0.5720	0.1745
8	0.4543	0.4537	0.1320
9	0.3595	0.3591	0.1112
10	0.2805	0.2803	0.0713
11	0.2108	0.2106	0.0948
12	0.1412	0.1412	0.0000

## VI. CONCLUSIONS

In this work, the implementation of the nonlinear dopant model was performed in an FPGA, demonstrating its functionality reproducing the voltage-current relationship of the memristor. In addition, this work shows a different methodology in the modeling and simulation of the memristor from which four advantages can be observed: 1) Design time is shorter, since the high level design is used which avoids the use of the hardware programming language, 2) Easy communication between the FPGA and Simulink, because the asynchronous serial interface that is used is transparent to the user 3) Simulink blocks can be used to define excitation signals and observe the results obtained, 4) With this methodology the use of floating-point arithmetic in an FPGA is simple allowing to obtain values similar to the numerical model. Finally, it is observed the importance of having a hybrid model of the memristor in order to analyze and design nonlinear analog circuits in general.

## REFERENCES

- [1] L.O. Chua, "Memristor-The missing circuit element," IEEE Trans. Circuit Theory, vol. 18, no. 5, pp. 507-519, Sep. 1971.
- [2] D.B. Strukov, G.S. Snider, D.R. Stewart and R.S. Williams, "The missing memristor found," Nature, vol. 453, pp. 80-83, May. 2008.
- [3] S.H. Jo, K.H. Kim, T. Chang, S. Gaba and W. Lu, "Si memristive devices applied to memory and neuromorphic circuits". In *Proceedings of 2010 IEEE International Symposium on Circuits and Systems (ISCAS)*, pp. 13-16, Jun. 2010.
- [4] R. Berdan, T. Prodromakis and C. Toumazou, "High precision analogue memristor state tuning," Electron. Lett, vol. 48, no. 18, August. 2012.
- [5] A. Wu, Z. Zeng and J. Chen, "Analysis and design of winner-take-all behavior based on a novel memristive neural network," Neural Comput & Applic, vol. 24, pp. 1595-1600, 2012.
- [6] I. Vourkas, V. Ntinias, G. Sirakoulis and A. Rubio, "A digital memristor emulator for FPGA-Based artificial neural networks". IEEE International Verification and Security Workshop (IVSW). Spain. doi: 10.1109/IVSW.2016.7566607
- [7] Y.N. Joglekar and S.J. Wolf, "The elusive memristor: Properties of basic electrical circuits," Eur. J. Phys, vol. 30, no. 4, pp. 661-675, Jul.2009.
- [8] T. Prodromakis, C. Papavassiliou, and C. Toumazou, "A versatile memristor model with nonlinear dopant kinetics," IEEE Trans. Electron Devices, vol. 58, no. 9, pp. 3099-3105, Sep.2011.
- [9] K. Zaplatilek, "Memristor modeling in Matlab & Simulink," In *Proceedings of the European Conference*. France, April 2011.
- [10] A.G. Radwan, M.E. Fouad, "Studies in Systems decision and control on the mathematical modeling of memristor, memcapacitor and memductor" Springer 2015.